

AD-A227 963

DTIC FILE COPY

②

8 Jun 87

Conference Presentation

Visualization of Three-Dimensional Flow Structures About a Pitching Forward Swept Wing

TA 2307-F1-38

J.B. Wissler, F.T. Gilliam, M.C. Robinson, J.M. Walker

F.J. Seiler Research Laboratory
USAF Academy CO 80840-6528

FJSRL-PR-90-0008

DTIC ELECTED
OCT 31 1990
S E D

Distribution Unlimited

Three-dimensional forced unsteady flow separation about a 30 degree forward swept wing was visualized for a constant pitch rate motion from zero to 60 degrees. The development of both wing tip and inboard leading edge vortices were observed with characteristics similar to those found in straight wing tests. The off-axis pitch geometry appeared to delay the initiation of the wing tip vortex to large angles of attack, indicative of a delayed lift response. the results are contrasted with previous straight wing findings using similar pitch motions and swept wing results obtained using sinusoidal motion histories.

flow visualization;
three dimensional flows;
flow separation.

10. NUMBER OF PAGES
10

11. PRICE CODE

12. LIMITATION OF ABSTRACT

UNCLASSIFIED

UNCLASSIFIED

UNCLASSIFIED

NONE

AIAA'87

Classified 5 Jun 89

AIAA-87-1322

Visualization of Three-Dimensional Flow Structures About a Pitching Forward Swept Wing

J. B. Wissler, F. T. Gilliam
Dept. of Aeronautics
U. S. Air Force Academy, Co.

M. C. Robinson
Dept. of Aerospace Engr. Sci.
Univ. of Colorado, Boulder, Co.

J. M. Walker
Frank J. Seiler Research Laboratory
U. S. Air Force Academy, Co.

Accession For	
NTIS	<input checked="" type="checkbox"/>
DTIC TAB	<input type="checkbox"/>
Unannounced	<input type="checkbox"/>
Justification	
By _____	
Distribution/ _____	
Availability Codes	
Dist	Avail and/or Special
A-1	

DISTRIBUTION STATEMENT A
Approved for public release; Distribution Unlimited

AIAA 19th Fluid Dynamics, Plasma Dynamics and Lasers Conference

June 8-10, 1987/Honolulu, Hawaii

Visualization of Three-Dimensional Structures

About a Pitching Forward Swept Wing

J.B. Wissler*
F.T. Gilliam**
Dept. of Aeronautics
U.S. Air Force Academy

M.C. Robinson***
Dept. of Aerospace Sciences
University of Colorado

J.M. Walker****
Frank J. Seiler Research Laboratory
U.S. Air Force Academy

Abstract

Three-dimensional forced unsteady flow separation about a 30° forward swept wing was visualized for a constant pitch rate motion from 0 to 60° . The development of both wing tip and inboard leading edge vortices were observed with characteristics similar to those found in straight wing tests. The off-axis pitch geometry appeared to delay the initiation of the wing tip vortex to large angles of attack, indicative of a delayed lift response. The results are contrasted with previous straight wing findings using similar pitch motions and swept wing results obtained using sinusoidal motion histories.

Nomenclature

c	wing chord	
\bar{R}	nondimensional rotational radius	R/c
t	time	
\bar{t}	nondimensional time	tV_∞/c
\bar{V}_r	nondimensional rotational velocity	V_r/V_∞
V_∞	freestream velocity	
α	angle of attack	
$\dot{\alpha}$	pitch rate	
α^*	nondimensional pitch rate	

Introduction

Forced unsteady flow separation is currently being investigated as a potential method to increase aerodynamic performance. The large transient lift and moment coefficients associated

with rapid excursions of an airfoil beyond static stall have been well documented.^{1,2,3,4,5,6} Hence, the potential exploitation of these forces as well as the potential adverse effects of envisioned "super-maneuverable" flight regimes continue to direct investigations into unsteady separation phenomena.

Previous research efforts have focused primarily on two-dimensional test configurations. Yet, the ultimate utility of these transient flows will depend upon the extent that two-dimensional flow field structures are found when three-dimensional geometries are used. In two-dimensional flows, the underlying physics which determine unsteady separation are not well understood. With three-dimensional test geometries, achieving a physical understanding is even more difficult due to the more complicated leading edge vortex structure and the interaction of the wing tip vortex.

Recent experimental investigations have provided some insight into dynamic stall vortex development created by forced flow separation about three-dimensional test models. Adler and Lutgtes⁷ found that three distinct flow regions existed above a sinusoidally pitched straight wing: a two-dimensional dynamic stall vortex dominated the flow inboard of 1.0 chords (1.0c) from the tip, a wing tip vortex dominated the flow over the tip, and a distinct region of strong vortex-vortex interactions existed over the airfoil between the wing tip and dynamic stall vortices. Robinson, et al,⁸ found the same behavior when a straight wing was pitched to high angles of attack at high constant pitch rates. The interaction region, however, extended further inboard with two-dimensional flow beginning at a position approximately 1.4 chords from the tip. On the other hand, vortex development over dynamically pitched delta wings is fundamentally different from that observed for straight wings. Gad-el-Hak and Ho^{9,10} found that for sinusoidally pitched delta wings, stationary vortices aligned with the leading edge resided over the wing upper surface. The diameter of the vortices increased and decreased with corresponding changes in angle of attack. Gilliam, et al,¹¹ investigated delta wings undergoing large amplitude constant pitch rate motions and found a strong interdependence between wing planform geometry and the flow structure. Additionally, three-dimensional influences were

* Capt, USAF, Instructor, Member AIAA
** Lt Col, USAF, Associate Professor, Member AIAA
*** Associate Professor Adjunct, Currently Visiting Professor, U.S. Air Force Academy, Member AIAA
**** Maj, USAF, Chief, Aeromechanics Division, FJSRL, Member AIAA

present everywhere on the wing from the onset of the pitch motion; no two-dimensional region existed.

Recent advances in composite structures and computer based flight control systems have made forward swept wings a viable design option for high performance aircraft. Forward sweep provides much of the same aerodynamic advantage as conventional sweep at high speed, and low speed characteristics are potentially better than those of conventionally swept wings.^{1,2} Previous investigations of pitching forward swept wings have considered low amplitude sinusoidal oscillations. Ashworth, et al,^{1,3} found that three distinct flow regions, similar to those found by Adler and Luttgies⁴, also existed on forward swept wings. But, more importantly from a performance perspective, the rapid separation and accompanying "cataclysmic stall" found in airfoil and straight wing tests was not observed with the forward swept wing.

The present investigation considers the flow field about a forward swept wing pitching to extremely high angles of attack (60°) at high constant rates. Smoke flow visualization was used to examine the initiation and development of both the leading edge and the wing tip vortices as functions of motion history and spanwise location. Comparisons of the resulting flow field development were made with previously tested wing geometries and motion histories.

Method

The flow visualization experiments were conducted at U.S. Air Force Academy in the Frank J. Seiler Research Laboratory 3' X 3' low speed wind tunnel. The forward swept wing was constructed from hollow NACA 0015 aluminum. The 6-inch chord airfoil stock was cut on both ends to form a 30 degree forward swept wing. The resulting model had an effective chord length of 6.93 inches. To enhance flow visualization, the wing was painted black with white reference marks at the leading and trailing edges placed at 0.2c increments along the span. The semi-span of the model was 11 inches. All tests were conducted with the pitch axis normal to the freestream flow direction and located 0.25 chords behind the leading edge of the root chord. A splitter plate along the wing root isolated the wing from tunnel wall effects.

A Locam II 16mm high speed movie camera operating at 200 frames per second recorded the pitching event and the ensuing flow field development. Illumination was provided by 3 Strobrite stroboscopic lights (7 μ s flash duration) synchronized with the camera. A smoke-wire located 12" upstream of the model produced the smoke used to visualize the unsteady flow development. An 18-inch tungsten wire (.005 inch diameter) suspended between two 0.25 inch copper rods could be positioned at any desired span location perpendicular to the wing axis. When coated with a commercial smoke producing fluid, small beads of fluid formed along the length of the wire. Application of a voltage across the wire, vaporized the fluid and produced a dense, planar sheet of smoke.

A programmable d.c. stepping motor connected to the wing via a 4 to 1 reduction gear controlled

the wing motion. Constant pitch rate motions were loaded into the stepper motor control card using a Masscomp 5500 data acquisition system. Actual angular displacements were measured during each run to ensure the prescribed pitch rate was achieved and that the pitching motion was smooth. Three nondimensional pitch rates were investigated: 0.2, 0.6, and 1.0 (actual pitch rates of 198, 594, and 991 deg/sec nondimensionalized by freestream velocity and the chord length). All tests were conducted at a free stream velocity of 10 ft/sec, with a corresponding chord Reynolds Number of approximately 27000.

Results

Flow visualization data provided both a qualitative and quantitative assessment of the flow field. Qualitative observations included trends in general flow structuring, identification of obvious interaction regions, circulation patterns, and characteristics of vortex development. With the use of a digitizing pad and the Masscomp data acquisition system, quantitative data, including leading edge vortex initiation angle, size, and location were also collected. An inertial reference frame was used to locate spatially dependent structures. The frame origin was located at the leading edge of the wing tip when the wing was at 0° angle of attack. The x-axis extended along the wing tip in the flow direction and the z-axis, denoting span location, extended inboard from the tip. All distances were nondimensionalized by the wing chord.

Overall View of the Pitching Event

Many of the same vertical structures observed in previous experiments with straight wings were found with the forward swept wing geometry. The chronology of vortex development can be seen in Figures 1 and 2 for the highest nondimensional pitch rate, $\alpha^+ = 1.0$. In Figure 1 the smoke sheet was introduced at a span location of 0.2c and the development of the wing tip vortex is clearly shown. Inboard leading edge or dynamic stall vortex development is documented in Figure 2 with smoke being introduced at 1.0c inboard of the tip. All photographs are temporally referenced to the initiation of the pitching motion with time being nondimensionalized by freestream velocity and the wing chord. A camera rate of 200 frames per second provides a nondimensional time of 0.087 between successive frames. Every other frame was printed in Figures 1 and 2 corresponding to a $\Delta \bar{t}$ between plates of 0.173.

As the wing began to pitch, flow on the bottom of the wing near the tip was directed out of plane and around the wing tip. The beginning of a flow discontinuity, or kink, in the smoke lines became visible on the underside of the wing (Figure 1, Col 1, Row 3). The kink in the smoke lines appeared to be a prelude to the formation of the wing tip vortex. At 40 to 45 degrees angle of attack (Figure 1, Col 1, Row 4-5) the flow discontinuity became the most prominent feature beneath the wing tip. Even at this large angle, no wing tip vortex is evident. As the wing reached maximum angle of attack (Figure 1, Col 2, Row 1-3), the flow discontinuity convected around the tip and was immediately swept up into the wing tip vortex.

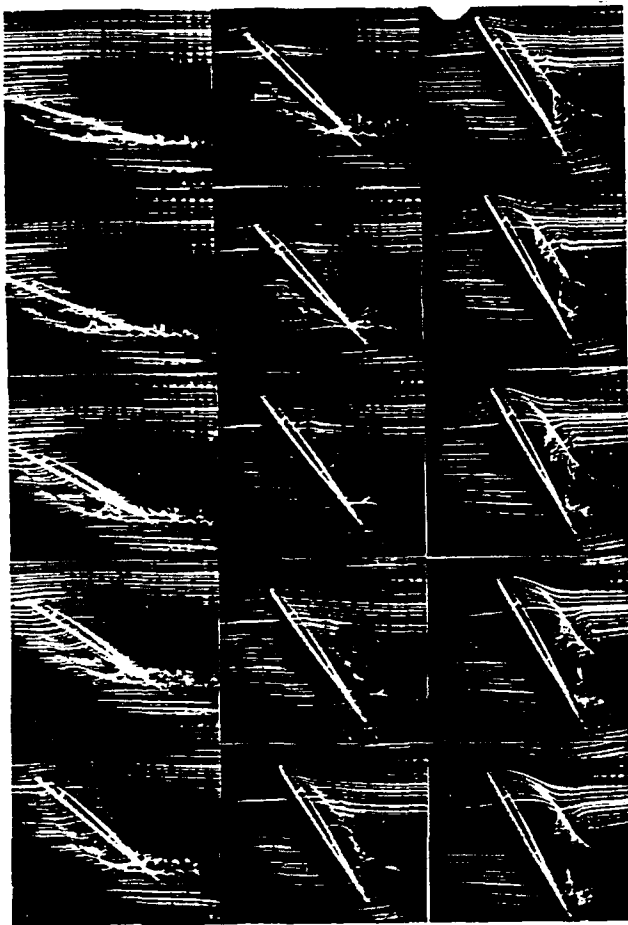


Figure 1. Vortex Development Near the Wing Tip,
 $\alpha^+ = 1.0$, $SL = 0.2c$, $\Delta \bar{\epsilon} = 0.173$.

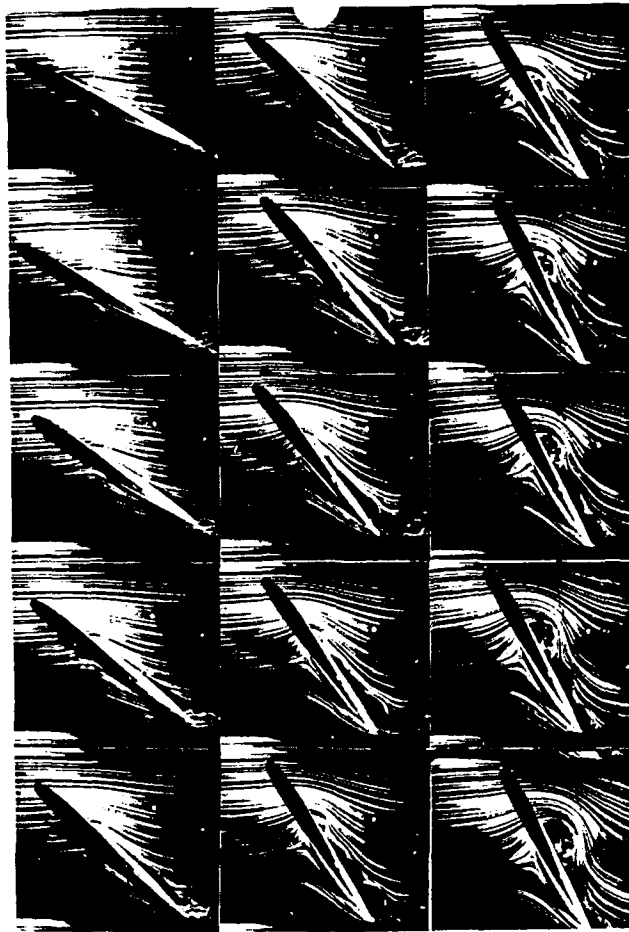


Figure 2. Leading Edge Vortex Development,
 $\alpha^+ = 1.0$, $SL = 1.0c$, $\Delta \bar{\epsilon} = 0.173$.

Vortex development further inboard of the wing tip was reminiscent of the structures observed in both two-dimensional and straight wing tests. Very little evidence of vortex development was observed until the wing approached maximum angle of attack. Then, a small separation region emerged near the leading edge (Figure 2, Col 2, Row 3) and developed into the leading edge vortex. Two other shear layer vortices were also present over the midchord and trailing edge.

Although Figures 1 and 2 show the flow development at one pitch condition ($\alpha^+ = 1.0$), the same general trends existed across test conditions. Changes in pitch rate, however, did alter specific attributes of the dynamic stall vortex development process.

Effects of Pitch Rate

As in previous investigations, nondimensional pitch rate had a direct influence on vortex development. Figures 3, 4, and 5 show the vortex development at span locations of $0.0c$, $0.6c$ and $1.0c$ respectively. In each figure, columns 1, 2, and 3 correspond to nondimensional pitch rates of 0.2 , 0.6 , and 1.0 . Photographs in each column are at 25° , 35° , 45° , 55° , and 60° from top to bottom. Hence the effects of pitch rate and span location may be compared directly across these three figures.

In the tip region (Figure 3), the flow was dominated by the wing tip vortex. The small kink in the smoke lines below the lower surface appeared at nondimensional pitch rates of 0.6 and 1.0 . This flow discontinuity was visible until the wing began to decelerate at the maximum angle of attack of 60° . The kink moved around the wing tip and wrapped into the forming helical tip vortex. As the tip vortex formed, the remnants of the kink were drawn down and into the vortex (Figure 3, Col 2-3). The largest discontinuity under the wing was found at the highest pitch rate, $\alpha^+ = 1.0$. Also, the merger of the discontinuity into the wing tip vortex was delayed at the highest pitch rate.

A most striking observation of the inboard flow development was the attached flow that existed to extremely high angles of attack (Figure 4). It was not uncommon to observe, particularly for the highest pitch rate, flow remaining attached for several picture frames after the wing reached 60° . Even for the lowest pitch rate ($\alpha^+ = 0.2$), flow attachment was still evident at angles of attack near 35° to 40° .

In conjunction with prolonged flow attachment, vortex initiation and growth were also delayed with increasing pitch rate. In Figures 3 and 4, vortex initiation, or at any given angle of attack vortex development, were delayed with increasing α^+ . The most dramatic effects occurred between $\alpha^+ = 0.2$

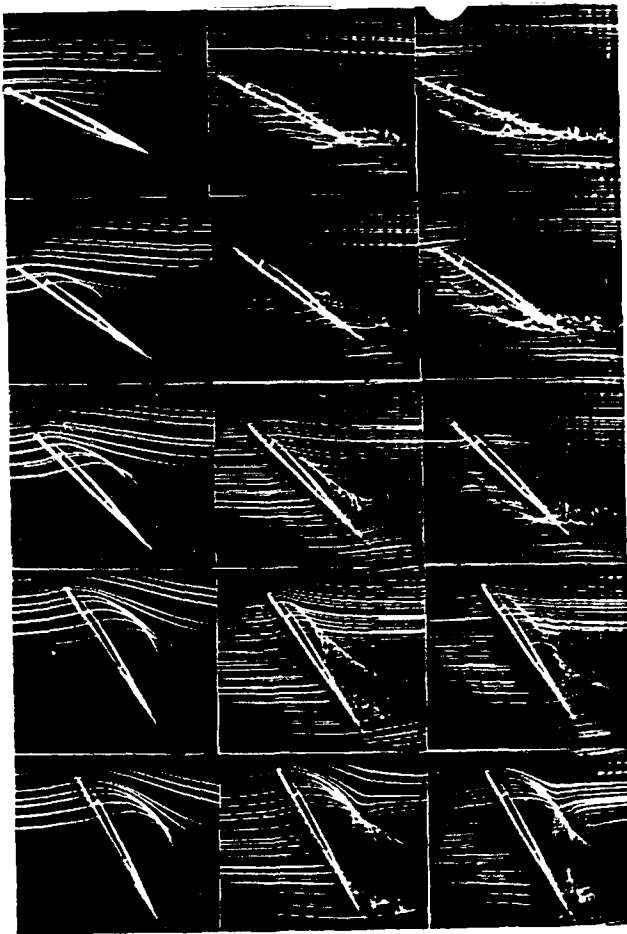


Figure 3. Wing Tip Vortex Development for Three Pitch Rates, $SL = 0.0c$, $\alpha^+ = 0.2, 0.6, 1.0$.

and 0.6 (Cols. 1 and 2). For an α^+ of 1.0, vortex initiation was delayed until the airfoil reached the maximum angle of 60° .

Following initiation, the subsequent growth and development of the leading edge vortex on the forward swept wing did not appear as cohesive as vortices observed in previous straight wing tests. At the lowest pitch rate tested ($\alpha^+ = 0.2$), multiple vortices initially appeared over the upper airfoil surface (Fig 4, Col 1, Row 1). These organized vortical structures rapidly broke down into what appeared as a "thickened" boundary layer over the upper surface of the wing. The first organized vortex to appear at the leading edge did not evolve into a dominant dynamic stall structure. Instead, the first vortex convected downstream and lost its cohesive structure in the "thickened" boundary layer. After the first vortex began to convect, a second vortex emerged behind the first. It was the second vortex which remained at the leading edge and experienced the growth, convection and shedding cycle indicative of dynamic stall. However, this dynamic stall vortex failed to produce the same energetic recirculation observed in straight wing experiments.

At faster pitch rates ($\alpha^+ = 0.6, 1.0$) vortex development also appeared somewhat tempered. Previous straight wing results have indicated very cohesive structuring of the inboard leading edge

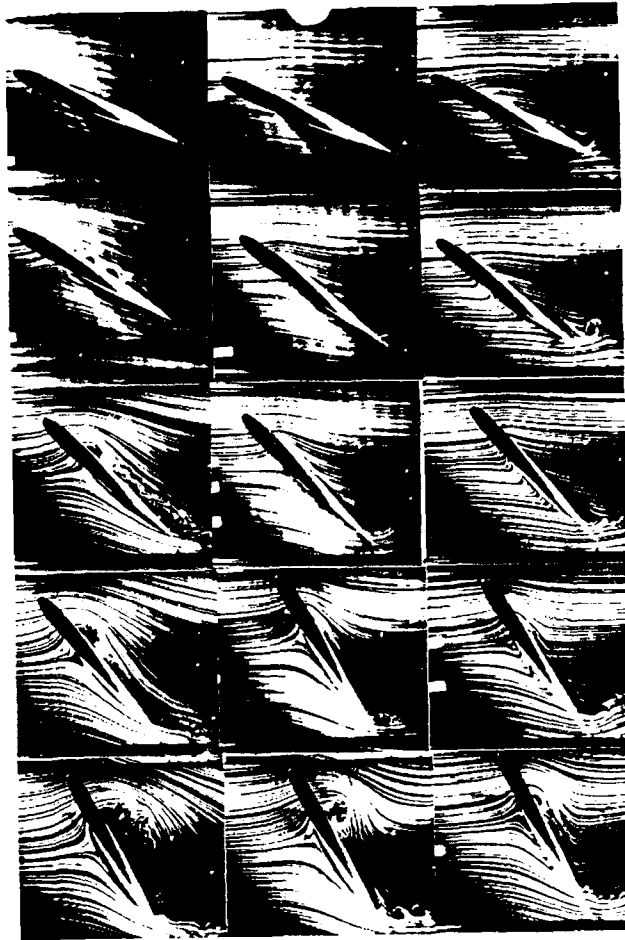


Figure 4. Mid-span Vortex Development for Three Pitch Rates, $SL = 0.6c$, $\alpha^+ = 0.2, 0.6, 1.0$.

vortex. Strong pressure gradients associated with these organized vortices were indicated in the large curvature of smoke lines down and around the vortex core. Vortex development over the forward swept wing fell short of the very energetic behavior seen in straight wing tests at equivalent test conditions.

Effect of Span Location

In Figures 4 and 5, span location influenced the development of the leading edge vortex. The most dramatic comparison can be made by contrasting the first column in the two figures. Span locations near the wingtip delayed vortex initiation and development. Equivalent angles of attack show much larger vortices inboard, away from the tip (Fig 5, Col 1). At an α^+ of 0.2 initiation of the leading edge vortex was delayed from 35 to 45° at span locations near the tip. Note the similarity in flow development between Col 1, rows 2 and 3 in Fig 4 and Col 1, rows 1 and 2 in Fig 5. After initiation (rows 3 and 2 in Figures 4 and 5 respectively) convection of the leading edge vortex was also delayed near the tip.

The spanwise flow development over the forward swept wing, when viewed from the rear, was generally similar to that of a straight wing geometry. Figures 6 and 7 document flow behavior at the wingtip ($0.0c$) and $0.6c$ inboard from the

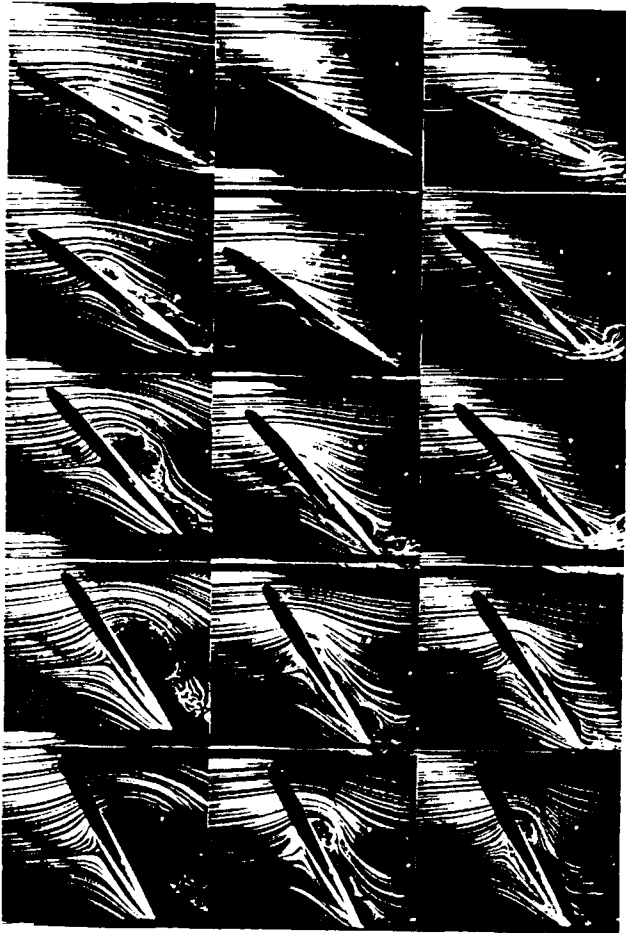


Figure 5. Inboard Vortex Development for Three Pitch Rates, $SL = 1.0c$, $\alpha^+ = 0.2, 0.6, 1.0$.

tip. Again the three columns correspond to α^+ values of 0.2, 0.6, and 1.0 while the rows show increasing angles of attack: 25, 35, 45, 55 and 59°.

Flow development about the wingtip was similar to that observed in previous large amplitude pitch motions.^{7,8,13} The tip region was dominated by the formation of a wing tip vortex over the upper surface. This vortex emerged as a conical structure (Fig 6) from the leading edge and extended inboard from the tip to approximately 0.8c. As noted in the previous side view figures, development of the wing tip vortex was delayed to large angles of attacks (approximately 45-55°) at high pitch rates ($\alpha^+ = 0.6, 1.0$).

Leading edge vortex initiation inboard (Fig 7) had very different characteristics than on rectangular wings. A quasi two-dimensional flow field inboard, away from tip effects, was found in previous straight wing tests but did not exist for the forward swept wing case. In general, the leading edge vortex initiated in a uniform line along the 30° swept forward edge. Soon after initiation, flow over the upper surface developed a span-wise flow component toward the wing root. On the lower surface, flow was pulled toward the tip. Inboard of a 0.4c span location, planar visualization cuts with the smoke sheet showed very little difference in development between span

positions. In fact, prior to vortex growth, span locations could not be distinguished from smoke patterns alone. Only at extremely high angles of attack, after the wing tip and leading edge vortex developed, could a span location be identified from smoke flow patterns. In straight wing visualizations, a clear demarcation line separated the two regions of wing tip and leading edge vortex development. This demarcation was nominally located along a line extending from the leading edge of the wing tip to a span location 0.8c inboard at the trailing edge. This distinct zoning of the flow field was not evident in the forward swept wing results.

Leading Edge Vortex Development

From the flow visualization sequences above, select points were digitized to help characterize the flow development. Figures 8, 9 and 10 plot the vortex diameter growth for different span locations at nondimensional pitch rates of 0.2, 0.6 and 1.0 respectively. Although the vortex diameter was based upon a qualitative "visual" assessment, only the trends in vortex behavior were considered important. Obtaining actual quantitative measures of vortex diameter were beyond the scope of this investigation.

In general, the leading edge vortex initiated first near the wing root and progressed toward the wing tip. This effect was most prominent at a nondimensional pitch rate of 0.2 (Fig 8). Initiation occurred first inboard (span location = 1.0c) at a non-dimensional time of $\bar{t} = 2.0$, relative to the onset of pitch motion. Near the tip, initiation was delayed to $\bar{t} = 3.0$. With increasing pitch rate (Figs 9 and 10) vortex initiation occurred earlier in the pitch motion ($\bar{t} = 1.5$) and the span dependence was not as great. At an α^+ of 1.0, initiation occurred along the leading edge within one camera frame.

The growth rate and vortex residence time over the wing behaved in a manner similar to straight wing and two-dimensional airfoil results. Leading edge vortices generated at $\alpha^+ = 0.2$ (Fig. 8) grew at a slower rate and resided over the airfoil for the greatest periods ($\Delta \bar{t} = 3.0$). At high pitch rates ($\alpha^+ = 1.0$, Fig 10) the initial growth rate was quite rapid inboard with an average duration of $\Delta \bar{t} = 1.5$.

Because of the diverse convection behavior of the leading edge vortex over the forward swept wing it was difficult to derive an average convection rate. At the tip, vortex convection was constrained while inboard convection proceeded in a uniform manner. Averaged convection rates at a span location of 1.2c were calculated at 35 and 50% of the freestream velocity for α^+ values of 0.2 and 1.0 respectively. Both the magnitudes of convective velocities and the dependence upon pitch rate were consistent with previous straight wing results at similar span locations.

Discussion

Forced unsteady separated flow about a forward swept wing possessed many of the same flow characteristics observed in previous experiments using different wing geometries and motion histories. In general, both a wing tip and a

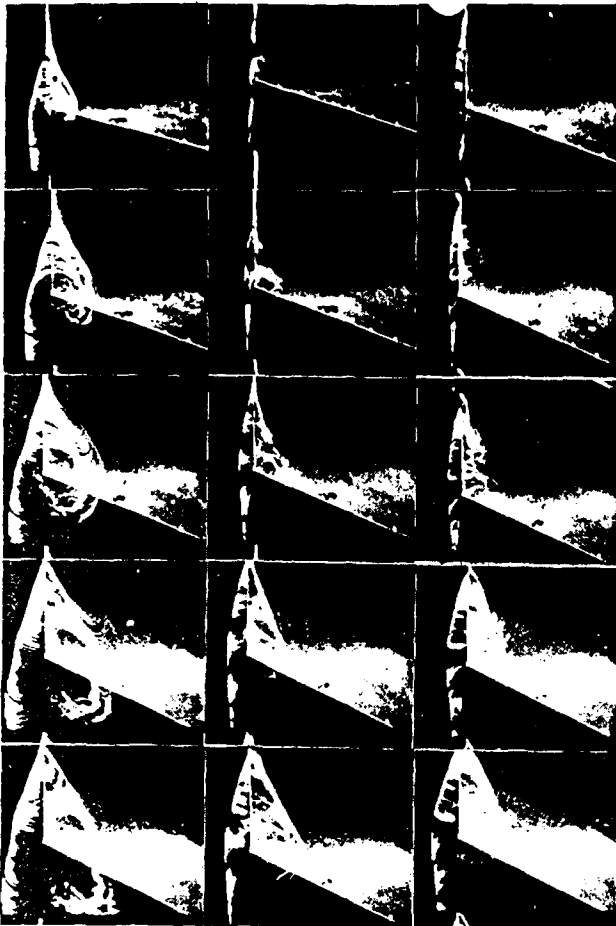


Figure 6. Rear View of Wing Tip Vortex Development, SL = 0.0c, $\alpha^+ = 0.2, 0.6, 1.0$.

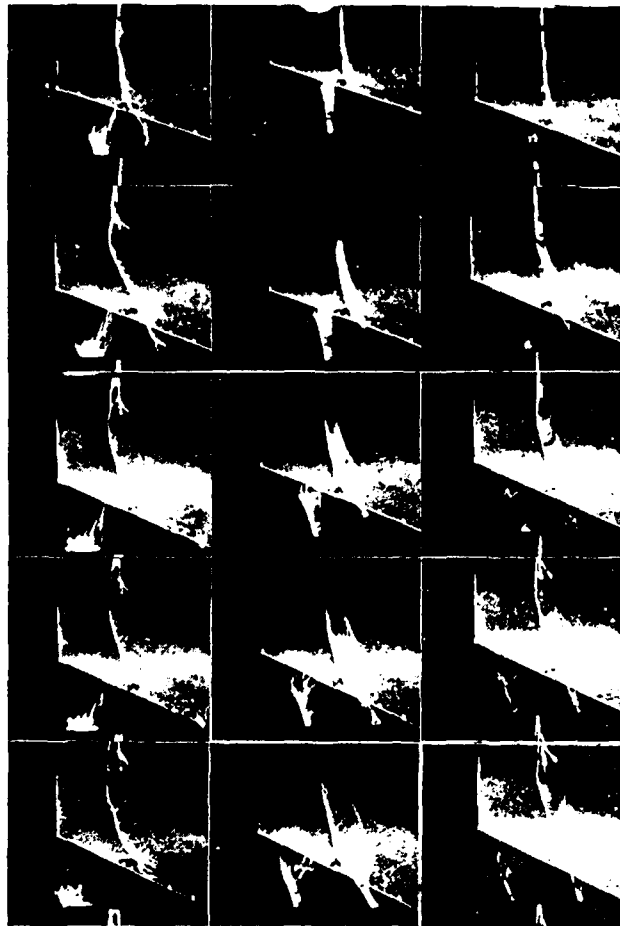


Figure 7. Rear View of Mid-Chord Vortex Development, SL = 0.6c, $\alpha^+ = 0.2, 0.6, 1.0$.

dynamic stall vortex were formed as the wing pitched beyond the static stall angle. The resulting flow field was affected by changes in the pitch rate and was dependent upon span location. The unique forward swept geometry also introduced some flow anomalies not previously observed.

Flow Attachment

Dynamic flow attachment observed in the current study was in many ways similar to the results reported by Ashworth, et al,¹³. Their static tests of a similar forward swept wing undergoing sinusoidal pitch oscillations indicated that separation occurred first inboard at 9° (at 1.0c) and progressed toward the tip as angle of attack increased (15° at 0.6c). With a sinusoidal motion of $15^\circ \pm 10^\circ$, no evidence of total flow separation was observed, but a dynamic stall vortex did initiate along the leading edge. This initiation was dependent on span location with earlier vortex development occurring inboard toward the root and delayed initiation at the tip.

These similarities are interesting given the difference in wing motion histories between the experiments. Ashworth, et al, used a pitch axis which paralleled the 30° forward swept wing at a distance of 0.22c from the leading edge. Also, the maximum angle attained (25°) with sinusoidal

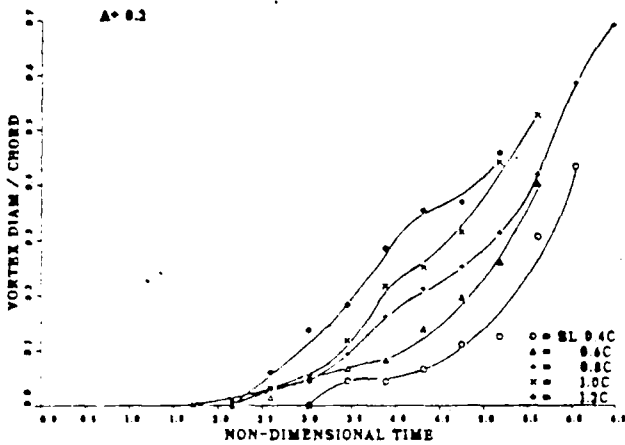
oscillations were substantially lower than the maximum angle used in the current tests (60°).

Differences in the degree of separation are more a function of the motion profile than maximum angle. Harmonic motions at modest rates continually force flow development through the oscillation angle. In contrast, single pitch tests at constant pitch rates permit the flow to separate during the relaxation period after motion ceases at the maximum angle of attack. Although flow development should be similar between harmonic and constant pitch motions at low rates (approaching quasi-steady), rapid harmonic motions produce extremely complicated multiple vortex environments from multiple oscillation cycles. In contrast, a rapid single pitch motion allows the dynamics of a single vortex event to be analyzed as a function of forcing rate.

Tip Flow

As observed in previous tests,^{7,8,13,14} formation of the wing tip vortex was derived from the vorticity accumulation on the lower wing surface. Displacement of the lower surface flow out and around the tip into the wing tip vortex has been documented independent of the wing geometry and motion history. Previous investigators^{7,13} have used the crossover angle between the wing tip

VORTEX DIAM VS N-D TIME



INDUCED ANGLE OF ATTACK

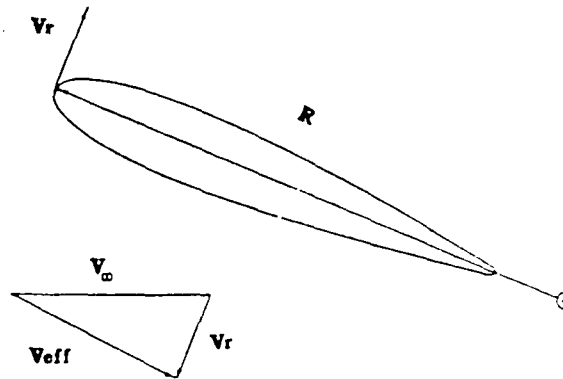
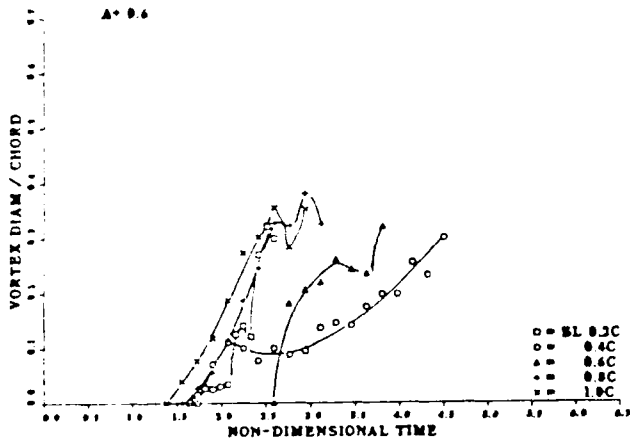
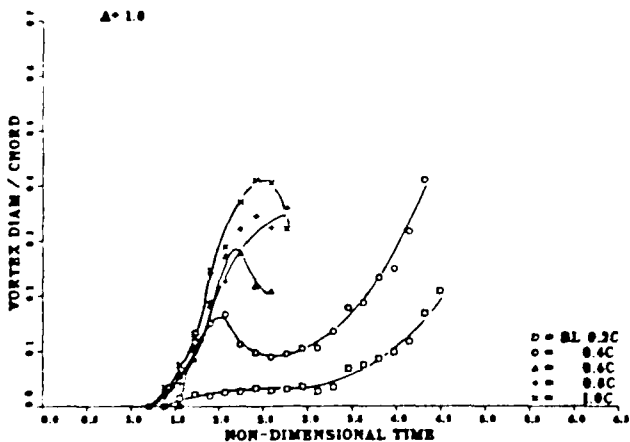


Figure 11. Induced Leading Edge Velocity

VORTEX DIAM VS N-D TIME



VORTEX DIAM VS N-D TIME



Figures 8, 9, 10. Vortex Initiation and Growth
 $\alpha^+ = 0.2, 0.6, 1.0$

and the helical wing tip vortex (β angle) as an indication of relative vortex strength. With sinusoidal motions, large variations in β were observed through the oscillation cycle for both straight and swept wing geometries. Constant pitch motions with a straight wing⁶ produced a constant angle of 90° (maximum angle possible) throughout the pitch motion. The same results were observed in these tests indicating, qualitatively, that a stronger wing tip vortex is generated with constant pitch rate motions to high angles of attack.

One anomaly not previously reported was the generation of the "kink" or flow discontinuity under the wing tip at high pitch rates ($\alpha^+ = 0.6, 1.0$). During the pitching motion, a wing tip vortex failed to develop until the forward swept wing was nearly at the maximum angle of attack. Concurrently, the flow discontinuity tracked beneath the wing tip until the same angle of attack was reached, convected around the wing tip and merged into the wing tip vortex. In contrast, previous straight wing tests⁶ with the same motion history at the same pitch rates had reported immediate formation of the wing tip vortex at the onset of the pitching motion independent of pitch rate.

The flow discontinuity may possibly be explained by the location of the pitch axis relative to the wing leading edge. Figure 11 shows a schematic of the induced leading edge velocity created by an angular rotation of the wing about the pitch axis. A simple relationship for the nondimensional induced leading edge velocity in terms of the nondimensional pitch rate and radius from the pitch axis can be expressed as:

$$\bar{V}_r = \alpha^+ \bar{R}$$

where \bar{R} is a linear function of span location. Rotational velocities near the wing tip become very large with increasing α^+ . Table 1 shows that the rotational leading edge velocity exceeds the freestream value of velocity at $\alpha^+ = 1.0$. At the onset of pitch ($\bar{t} = 0^+$) instantaneous values of the induced angle of attack are large in negative values as seen in Table 2.

Table 1. Rotational Velocity, \bar{V}_r , at the Wing Tip

α^+	LE	Midchord	TE
	$\bar{R}=1.043$	$\bar{R}=0.543$	$\bar{R}=0.043$
0.2	0.209	0.109	0.0085
0.6	0.626	0.326	0.0255
1.0	1.043	0.543	0.043

Table 2. Induced angle of attack, α_i (deg)

α^+	LE	Midchord	TE
0.2	-11.8	-6.2	-0.5
0.6	-32.1	-18.1	-1.5
1.0	-46.2	-28.5	-2.5

From these test conditions relatively low static pressures could have been created beneath the wing. The impulsive rotation of the wing could so dominate the flow field that a positive pressure difference was temporarily created on the upper wing surface despite the growing positive angle relative to the freestream velocity. And, because of the counterbalancing influences on the effective angle of attack, unsteady separation failed to develop near the wing tip during the early stages of the pitch motion. The "kink" suggests that a low pressure region beneath the tip did exist temporarily. This hypothesis is reinforced by the increasing clarity and strength of the disturbance as pitch rate increased. Also, the absence of a discernible wing tip vortex suggests that the pitched forward swept wing was not producing lift in the tip region until very large angles were achieved. In fact, negative lift may have been produced early in the pitch cycle, with the "kink" indicating a negative wing tip vortex development. Rapid translation of the flow discontinuity around the wing tip may have signalled the change from negative to positive lift generation.

Vortex Initiation and Growth

Leading edge vortex initiation and subsequent development appeared more capricious than previous straight wing investigations. A greater sensitivity to nondimensional pitch rate and span location influences produced vortices with unique characteristics. At low pitch rates initiation of the dynamic stall vortex was preceded by two different events. First, the formation and breakdown of multiple vortices over the wing followed by the initiation of a small vortex over the leading edge which preceded the dynamic stall vortex. Similar multiple vortex structuring had been reported by Ashworth, et al,¹³ in their sinusoidal investigations of forward swept wing phenomena. At these lower pitch rates, vortex initiation was sensitive to span location with separation and subsequent vortex initiation occurring first near the wing root and progressing toward the wing tip.

In contrast, high pitch rates tended to focus the vorticity distribution over the wing into a single separation event. The dynamic stall vortex initiated almost simultaneously along the leading edge in a single well defined structure. The vortex diameter growth as a function of nondimensional time for high pitch rates (Figure 10) indicated an interesting behavior. Vortex initiation and early growth occurred in a nearly uniform manner along the span. After the initial rapid growth, a decrease in diameter was observed first near the tip and successively toward the root.

This behavior can be correlated with a visual change in the leading edge vortex. The rapid growth period exhibited a nearly two-dimensional structuring in vortex development. The diameter decrease occurred when the vortex structure deteriorated with three-dimensional cross flow toward the wing root. This same behavior had been observed in straight wing experiments under duplicate test conditions. Even though a significantly different test geometry was used in this experiment, almost duplicate initiation and two-dimensional duration times were recorded for equivalent pitch rates and span locations. Qualitatively, however, the strong pressure gradient influences indicated by the substantial potential flow entrainment around the vortex core in the straight wing tests were not as pronounced in these results.

Conclusions

Forced unsteady flow separation about a forward swept wing produced many of the same flow structures observed in previous straight wing and oscillating forward swept wing investigations. Two dominant vortices were generated, around the wing tip and inboard over the wing leading edge. Initiation and development of the leading edge vortex was dependent upon both span location and nondimensional pitch rate. The most dramatic effect was found at large pitch rates where span influences collapsed to uniform initiation and growth. Ultimately, three-dimensional breakdown of the leading edge vortex occurred, analogous to the behavior observed in straight wing tests.

The off-axis pitch geometry did provide one flow anomaly not previously reported. Initiation of the wing tip vortex was delayed to significantly higher angles of attack. A flow discontinuity beneath the wing appeared as a prelude to wing tip vortex initiation. It is not clear whether the flow "kink" was in response to a low pressure region beneath the wing tip, or resulted from some other response to the dynamic pitching motion. Future investigations using an instrumented pressure airfoil will examine the magnitude of the vortex induced pressure fields about the wing and resolve the issues of overall lift versus wing tip vortex development.

The relative importance of this geometry in current aircraft design makes the swept forward wing a prime candidate for investigation of "supermaneuverable" flight responses to forced unsteady flows. These preliminary findings suggest that the unsteady response for this wing planform and motion history may not be as advantageous as some other combinations that have been tested.

However, further quantitative measures should provide additional insight into both application and utility of this design in forced unsteady environments.

References

1. McCroskey, W.J., "Unsteady Airfoils", Annual Review of Fluid Mechanics, 1982, pp 285-311.
2. McCroskey, W.J., "Some Current Research in Unsteady Fluid Dynamics", The 1976 Freeman Scholar Lecture, Journal of Fluids Engineering, Vol 99, 1977, pp 8-38.
3. Carr, L.W., K.W. McAlister, and W.J. McCroskey, "Analysis of the Development of Dynamic Stall based on Oscillating Airfoil Experiments", NASA TN-8382, Jan 1977.
4. Carr, L.W., "Dynamic Stall Progress in Analysis and Prediction," AIAA Paper 85-1769, Snowmass, CO, Aug 1985.
5. Jumper, E.J., S.J. Shreck, and R.L. Dimmick, "Lift-Curve Characteristics for an Airfoil Pitching at Constant Rate," AIAA Paper 86-0117, Reno, NV, Jan 1986.
6. Walker, J., H. Helin, and D. Chou, "Unsteady Surface Pressure Measurements on a Pitching Airfoil," AIAA Paper 85-0532, Boulder, CO, March, 1985.
7. Adler, J.N. and M.W. Luttses, "Three-Dimensionality in Unsteady Flow About a Wing," AIAA Paper 85-0132, Reno, NV, Jan 1985.
8. Robinson, M., H. Helin, F. Gilliam, J. Russell, and J. Walker, "Visualization of Three-Dimensional Forced Unsteady Flow," AIAA Paper 86-1066, Atlanta, GA, May, 1986.
9. Gad-el-Hak, M. and C.-M. Ho, "The Pitching Delta Wing," AIAA Journal, Vol 23, Nov 1985.
10. Gad-el-Hak, M. and C.-M. Ho, "Unsteady Vortical Flow Around Three-Dimensional Lifting Surfaces," AIAA Journal, Vol 24, May, 1986.
11. Gilliam, F.T., J.B. Wissler, J.M. Walker, and M.C. Robinson, "Visualization of Unsteady Flow about a Pitching Delta Wing," AIAA Paper 87-0240, Reno, NV, Jan 1987.
12. Moore, M. and D. Frei, "X-29 Forward Swept Wing Aerodynamic Overview," AIAA Paper 83-1834, Danvers, MA, July, 1983.
13. Ashworth, J., M. Waltrip, and M.W. Luttses, "Three-Dimensional Unsteady Flow Fields Elicited by a Pitching Forward Swept Wing," AIAA Paper 86-1104, Atlanta, GA, May, 1986.
14. Freymuth, P., "The Vortex Patterns of Dynamic Separation: A Parametric and Comparative Study", Progress in Aeronautical Science, Vol 22, 1985, pp 161-288.